Continental Shelf Research 204 (2020) 104175

Contents lists available at ScienceDirect

Continental Shelf Research

journal homepage: http://www.elsevier.com/locate/csr

Air-sea CO_2 flux in an equatorial continental shelf dominated by coral reefs (Southwestern Atlantic Ocean)

Luiz C. Cotovicz Jr. *, Raisa Chielle, Rozane Valente Marins

Instituto de Ciências do Mar (LABOMAR), Universidade Federal do Ceará, Fortaleza, Ceará, Brazil

ARTICLE INFO

Keywords:
Carbon dioxide
Carbonate system
Coral reefs
Equatorial continental shelf
Southwestern atlantic ocean

ABSTRACT

Coral reefs are ecosystems highly vulnerable to changes in seawater carbonate chemistry, including those related to the ocean acidification and global warming. Brazilian coral reefs contains the major area of reefs coverage in the Southwestern (SW) Atlantic Ocean, however, studies aimed at investigating the controls of seawater carbonate chemistry in coral reefs are still overlooked in Brazil. This study comprehends the first investigation of complete seawater carbonate chemistry parameters in a section of the equatorial continental shelf dominated by coral reefs in the SW Atlantic Ocean. The sampling included spatial continuous underway measurements of sea surface CO_2 fugacity (fCO_2sw), temperature (SST), salinity (SSS), and discrete investigations of total alkalinity (TA), dissolved inorganic carbon (DIC), bicarbonate (HCO_3^-), carbonate (CO_3^{2-}), and saturation state of aragonite (Ω_{ara}). The study was conducted during a dry period (July-2019) in the Marine State Park of *Pedra da Risca do Meio* (PRM), a marine protected area dominated by coral reef communities. Overall, the coral-reef dominated waters presented higher values of fCO_2sw (475 ± 28 μatm), and lower values of pH_T (7.98 ± 0.008), CO_3^{2-} (217 ± 5 μmol kg^{-1}) and Ω_{ara} (3.49 ± 0.07), compared to nearshore regions without the influence of coral reef waters, where the averages of fCO_2sw, pH_T, CO_3^{2-}, and Ω_{ara}were, respectively, 458 ± 21 μatm, 8.00 ± 0.007, 224 ± 4 μmol kg^{-1}, and 3.58 ± 0.05. The relationship between salinity-normalized TA (nTA) and salinity-normalized DIC (nDIC) showed a slope higher than 1 (1.26) in the coral reef, evidencing the occurrence of calcium carbonate ($CaCO_3$) precipitation and prevalence of inorganic carbon metabolism. The $CaCO_3$ precipitation involves the consumption of TA and DIC in a ratio 2:1, with production of CO_2. This mechanism explains the higher values of fCO_2sw in the coral reef-dominated waters. The values of fCO_2sw were always higher than the atmospheric values (fCO_2air), indicating a permanent source of CO_2 in the study area during the sampled period. The calculated fluxes of CO_2 at the air-sea interface averaged 8.4 ± 6.5 mmolC m^{-2} d^{-1} in the coral reef-dominated waters, and these data are higher than those verified in nearshore and offshore locations. These higher emissions of CO_2 in coral reef-dominated waters evidence that the carbon budgets calculated for North and Northeastern continental shelf of Brazil must include these environments taking into account the widespread coral reef coverage in the region. This study also confirms that biogeochemical processes occurring in coral reefs are modifying the seawater carbonate chemistry, with implication in the context of the current process of ocean acidification.

1. Introduction

The anthropogenic activities, mainly the burning of fossil fuels and land use changes, are increasing the rates of CO_2 emissions to the atmosphere (IPCC, 2013). The actual atmospheric concentration of CO_2 surpassing 410 ppm is unprecedented over the past 3 million years (Willeit et al., 2019). This high amount of CO_2 in the atmosphere is of global concern, because CO_2 is the principal anthropogenic greenhouse gas and is associated to the increase of global atmospheric temperature (IPCC, 2013). Since the pre-industrial Revolution, the oceans absorbed about 20–30% of the anthropogenic CO_2 emissions (Feely et al., 2004; Le Quéré et al., 2018). When CO_2 dissolves in the water, it produces carbonic acid (H_2CO_3), which ionizes releasing hydrogen ions (H^+) and lowering the pH (Hoegh-Gulberg et al., 2017). The pH controls the composition of the (DIC) species in seawater. DIC is composed of dissolved CO_2 (CO_2aq), and the anions HCO_3^- and CO_3^{2-} (Dickson, 2010). For very low values of pH (<5), the CO_2aq is the predominant specie, however, for typical oceanic conditions (pH = ~8.10), the HCO_3^- is

* Corresponding author.
E-mail address: lccjunior@id.uff.br (L.C. Cotovicz).

https://doi.org/10.1016/j.csr.2020.104175
Received 18 December 2019; Received in revised form 3 June 2020; Accepted 6 June 2020
Available online 23 June 2020
0278-4343/

predominant, followed by CO_3^{2-} and CO_2aq. As more CO_2 hydrates, more H^+ is released in the water, decreasing the pH and the concentration of CO_3^{2-}, and increasing the concentrations of HCO_3^- and CO_2aq (CO_2aq is proportional to seawater fugacity of CO_2; fCO_2sw). These changes in the seawater carbonate chemistry linked to the uptake of anthropogenic CO_2 by the oceans are referred as the process of ocean acidification, considered the "other CO_2 problem" (Doney et al., 2009; Gattuso et al., 2015).

Despite the fact that the oceans are a net sink of CO_2, the distributions of fCO_2sw and associated air-sea fluxes are highly heterogeneous in the global surface oceans reflecting the different climate domains (Takahashi et al., 2002, 2014). This heterogeneity is larger in coastal zones, where the diverse sources and sinks of carbon and their interactions remain poorly understood (Bauer et al., 2013). Overall, continental shelves act as a sink of CO_2 of about 0.25–0.45 Pg C yr^{-1} (Borges, 2005; Borges et al., 2005; Cai, 2011). There is a marked latitudinal influence. Continental shelves at high and temperate latitudes are sinks of CO_2, in contrast to subtropical and tropical that are sources of CO_2 to the atmosphere (Borges, 2005; Borges et al., 2005). The up-scaling of air-water CO_2 fluxes is still hampered not only due to the poorly resolution at spatial and temporal scales, but also because continental shelves are increasing global sink for atmospheric CO_2 (Laruelle et al., 2018). The sink of CO_2 promoted by the continental shelves can be compensated by the emissions from nearshore coastal ecosystems, at about 0.10 to 0.40 Pg C yr^{-1}. (Borges et al., 2005; Cai, 2011; Chen et al., 2013). These carbon exchanges at air-water interface, in addition to the important inputs of TA and DIC from river sources, wetlands, and high rates of primary productivity, respiration and carbon burial, indicate the significance of this biogeochemically active region in the global CO_2 cycle (Borges, 2005; Cai, 2011; Bauer et al., 2013).

The presence of coral reefs on continental shelves can affects the air-water CO_2 fluxes due to the occurrence of $CaCO_3$ precipitation in these environments (Frankignoulle and Gattuso, 1994). The production of carbonate-containing structures is high in warm-water coral reefs (Hoegh-Guldberg et al., 2017). The reaction of carbonate precipitation can be write as:

$$Ca^{2+} + 2HCO_3^{2-} = CaCO_3 + CO_2 + H_2O \tag{1}$$

The precipitation of $CaCO_3$ by marine organisms releases CO_2 in the water. For this reason, coral reef-dominated habitats are considered sources of CO_2 to the atmosphere (Gattuso et al., 1999). Coral reefs release ~ 0.005 to 0.08 Gt C as CO_2 annually (Ware et al., 1992; Borges et al., 2005), with emissions averaging 1.51 mol C m^{-2} yr^{-1} (Borges et al., 2005). However, it must be highlight that these estimates are based on few ecosystems. Note that the reaction of carbonate precipitation also comprises alteration in TA and DIC of seawater, i.e., TA and DIC are changed in a ratio of 2:1 for every mole of $CaCO_3$ precipitated, considered the inorganic metabolic pulse of corals (Cyronak et al., 2018). The concentrations of dissolved CO_2, TA and DIC in coral reefs are also altered by biogeochemical processes linked to the organic metabolic pulse by the processes of photosynthesis and respiration (Xue et al., 2016; Cyronak et al., 2018). High temporal resolution observations in coral reef-dominated waters also revealed that these ecosystems can shift from undersaturated conditions with respect to the atmosphere to oversaturated conditions following seasonal tendencies due to a combination of thermal, biological and mixing effects (Xue et al., 2016). However, as the major part of coral reef ecosystems are net sources of CO_2, the net inorganic metabolism (net community calcification, NCC) are frequently more important than the net organic metabolism (net community production of organic matter, NCP) (Cyronak et al., 2018).

Warm-water coral reefs are susceptible to the negative effects of global ocean changes, particularly extreme seawater temperatures and ocean acidification (Gattuso et al., 2015). The decrease of pH is associated to the decrease of $CaCO_3$ saturation state of seawater (Ω), which predicts the thermodynamic tendency to occur net precipitation of $CaCO_3$ ($\Omega > 1$) or net dissolution ($\Omega < 1$) (Dickson, 2010).The aragonite is more important in shallow coral reef environment (Morse et al., 2007; Mucci, 1983). This mineral is essential to many phytoplankton and benthic species, and also abundant in coral reef habitats that are dominated by immobile, calcifying organisms (Gattuso et al., 2015). In addition, marine heat waves have already resulted in large-scale coral bleaching and mortality events (Hughes et al., 2017; Hoegh-Guldberg et al., 2017; IPCC, 2019). Indeed, recent studies have been shown that marine heat waves combined with decline of pH could alter the global habitat suitability for shallow coral reef ecosystem (Couce et al., 2013). The last report of the Intergovernmental Panel on Climate Change (IPCC) argued that coral reefs are already at high risk with "very high confidence" at current levels of warming (IPCC, 2019). In addition, it is "virtually certain" that the ocean pH is declining by associating $CaCO_3$ dissolution, leading to community changes (Agostini et al., 2018; IPCC, 2019).

Despite this extreme vulnerability of coral reef ecosystems in light of these global changes of seawater carbonate chemistry, this thematic is overlooked in the South Atlantic Ocean. To our best knowledge, there are not yet studies investigating air-sea CO_2 fluxes and carbonate chemistry properties in coral reef-dominated waters in the South Atlantic Ocean. The Southwestern Equatorial region of the South Atlantic hold poorly studied coral reef-dominated waters of important scientific interest. Large portions along the North and Northeast Brazilian coast host shallow-water coral assemblages on sandstone (Knoppers et al., 1999; Leão et al., 2016; Soares et al., 2017), in addition to the recent mapped Mesophotic Coral Reef Ecosystems (MECs) underneath the Amazon River Plume (Moura et al., 2016). In this study, the air-sea fluxes of CO_2 and carbonate chemistry were investigated in a marine protected area located in the Brazilian Equatorial Northeast Shelf (Fig. 1). The vast majority of studies investigating atmospheric CO_2 exchanges in coral reef waters were conducted in very shallow ecosystems (atolls, intertidal environments) (Bates et al., 2001). The coral reefs of *Pedra da Risca do Meio* (PRM) are located at depths varying between 14-40 m, which is much deeper than most documented studies. Our main hypothesis is that the presence of coral reefs at such depths will alter the carbonate chemistry in surface waters due to the benthonic precipitation of $CaCO_3$ (prevalence of inorganic metabolic pulse). The reef data will present higher concentrations and emissions of CO_2 compared to adjacent and offshore waters non-dominated by coral reef habitats.

2. Material and methods

2.1. Study area

The study area is the Marine State Park of Pedra da Risca do Meio (PRM), a marine protected area located at 23 km off Fortaleza city (Fig. 1). The PRM (03°33'80''- 03°36'00''S and 038°21'60''- 038°26'00''W) has a superficial area of 33.2 Km^2, with depths varying between 18 and 25 m and sheltered by submerged tropical coral reefs (Soares et al., 2011, 2019). The region is dominated by coral reef communities, particularly the scleractinian or hard corals, such as *Siderastrea stellata* Verrill, and low abundances of *Montastraea cavernosa* Linnaeus and *Mussismilia hispida* Verrill (Soares et al., 2019). The sediments are composed mainly by gravel and sand, with high aggregation of calcareous algae (Soares et al., 2011). The submerged rock formations present between 1 and 3 m of height with linear arrangement (Soares et al., 2011). The PRM presents 12 of these linear rock formations, with variable length and width.

The continental shelf of the State of Ceará is shallow, has a reduced width (60–80 km), holds high SST (25–30°C), and high SSS (30–38) (Knoppers et al., 1999; Behling et al., 2000). Specifically for the PRM region, the annual average of SST is about 27°C, whereas for SSS the annual average is about 36 (Soares et al., 2019). The region presents a semi-arid equatorial climate, with a small and sparse fluvial drainage

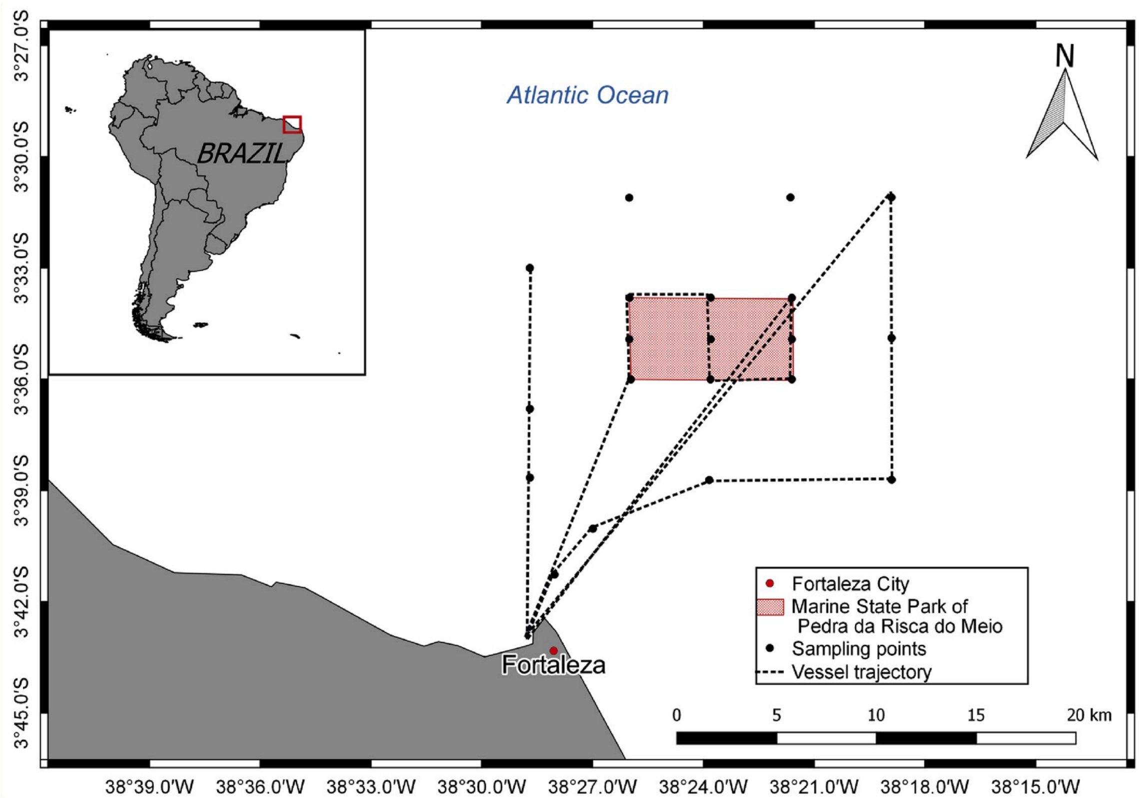

Fig. 1. Location of "*Parque Estadual Marinho da Pedra da Risca do Meio* (PRM)" - Equatorial SW Atlantic Ocean, Brazil (red rectangle). The figure also shows the location of discrete sampling stations (black dots), the cruise tracks of the vessel with continuous measurements (dotted lines), and Fortaleza City (red dot). (For interpretation of the references to colour in this figure legend, the reader is referred to the Web version of this article.)

(Marques et al., 2008). The ocean circulation in the region is dominated by the North Brazil Current (NBC), which originates from the bifurcation of the South Equatorial Current (SEC) between 2°S and 12°S (Silveira et al., 1994). The narrow and open shelf is almost entirely covered by carbonate sediments due to little freshwater input (Knoppers et al., 1999). The seaward transport of land-derived materials in this region can be considered minor as inferred from the relatively low sediment yields of the watersheds, low concentrations of suspended matter, and predominance of carbonate sediments (Knoppers et al., 1999).

2.2. Sampling strategy

The sampling was conducted between 08/07/2019 and 11/07/2019, historically considered as the dry period. Spatial surveys were conducted with transects leaving from the Mucuripe Port (Fortaleza city) until the Marine Protected Area, covering adjacent localities (Fig. 1). A medium size oceanographic vessel (Argo Equatorial) was used for the spatial surveys, with departures in the morning, and arrivals in the afternoon. Along the boat tracking, continuous and discrete seawater measurements were performed. Continuous and online measurements were conducted for date and time of geographical position, partial pressure of CO_2 (pCO_2sw), salinity, temperature and wind velocity. Surface seawater was sampled on discrete points distributed regularly along the transects for TA and chlorophyll *a* (Chl *a*) concentrations (Fig. 1).

2.3. Continuous measurements

The design and mode of operation of the semi-autonomous continuous measurement system is based on Pierrot et al. (2009) and well-described by Carvalho et al. (2017). Briefly, a water pump placed at a depth of about 1.0 m provided continuous seawater flow (~6 L min^{-1}) to the vessel. One part of the water flux (~2.5 L min^{-1}) was directed to a thermosalinograph (SeaBird Electronics®) that recorded the SST and SSS. After passing by the thermosalinograph, the water flow was directed to an equilibration system equipped with two equilibrators "shower head type" and a Non-Dispersive InfraRed gas analyser (NDIR) for CO_2 quantification (Licor-7000®CO_2/H_2O gas analyser). The CO_2 quantification in the gas phase was free from humidity. The molar fraction of CO_2 in dry air (xCO_2 ppm) measured in the equilibrator (xCO_2eq) was converted to the seawater partial pressure of CO_2 (pCO_2) according:

$$pCO_2eq = (P - pH_2O) * (xCO_2eq) \quad (2)$$

where P is the pressure in the equilibrator (assumed to be the same of atmospheric pressure) and pH_2O is the pressure of water vapor (atm), taken from Weiss and Price (1980). The fugacity of CO_2 (fCO_2 in μatm) was calculated from the pCO_2 values in the headspace gas that is proportional to the concentration of CO_2 using the temperature of the equilibrator, atmospheric pressure and the viral coefficients for CO_2 (Weiss, 1974), as follows:

$$fCO_2eq = pCO_2eq * \exp((B + 2\delta)P/RT) \quad (3)$$

Where B = -1636.75 + (12.0408*T) – (0.0327957*T^2) + (0.0000316528*T^3), R is the gas constant, T is the equilibrator temperature (Kelvin), and δ = 57.7–0.118xT. The temperature measured in the surface seawater and equilibrator were slight different, then a correction was applied to compensate such difference. The empirical temperature dependence used was proposed by Takahashi et al. (1993), according:

$$fCO_2sw = fCO_2eq * \exp(0.0423x(SST - Teq)) \quad (4)$$

WherefCO_2sw represents the seawater fugacity of CO_2 at *in situ* conditions. The system was calibrated within cycles of 6 h using air free CO_2 by passing N_2 in the NDIR followed by standard gases with nominal concentrations of 280.6 ppm, 362.2 ppm and 500.9 ppm (White Martins Certified Gases Concentrations). After every 6 h, atmospheric fCO_2 measurements (fCO_2air) were also performed with air taken from the top of the vessel at 10 m high. The accuracy of the fCO_2sw measurements was estimated at about ±2 µatm. The wind velocity was measured with an anemometer model Davis S-WCF-M003 applying corrections for the vessel velocity and direction of navigation. The records from parameters measured continuously, including the date and time of geographical position, vessel velocity, SST, SSS, fCO_2sw, water content in the detector and wind velocity are averaged at a frequency of 1 min.

2.4. Discrete measurements and laboratory analysis

Discrete samples were collected at a depth of ~1 m in selected positions (Fig. 1) using the continuous water flow, and then conditioned for further chemical analysis in laboratory (i.e. fixed and/or kept on ice in the dark). The water was filtered with Whatman® Grade GF/F Glass Microfiber filters (pre-combustion at 500 °C for 6 h), followed by determination of TA and Chl *a*. The filters for analysis of Chl *a* were kept at −18 °C prior to analysis. The TA measurements were performed with the classical Gran (1952) titration with an automated titration system (Metler Toledo model T50) in filtered water samples. The accuracy of this method was ±4 µmol kg^{-1} (inferred from certified reference material CRM, A. G. Dickson from Scripps Institution of Oceanography). Chl *a* was extracted from the filters with 90% acetone and quantified by spectrophotometry according to Strickland and Parsons (1972). The oxygen was measured with a calibrated YSI Professional Plus multiparameter probe.

2.5. Calculations

2.5.1. Carbonate system

The pH_T (on the total scale), DIC, HCO_3^-, CO_3^{2-} and Ω_{ar} were calculated from fCO_2sw, TA, SST, and SSS using the CO2calc 1.2.9 program (Robbins et al., 2010). We used the dissociation constants for carbonic acid proposed by Mehrbach et al. (1973) refitted by Dickson and Millero (1987), the borate acidity constant from Lee et al. (2010), the dissociation constant for the HSO_4^- ions from Dickson (1990) and the CO_2 solubility coefficient of Weiss (1974). The solubility product of aragonite in seawater was taken from Mucci (1983) and the concentrations of calcium (Ca^{2+}) were assumed proportional to the salinity (Millero, 1979). Even taking account the occurrence of $CaCO_3$ precipitation in the study area, the impact of this process on the Ca^{2+}/salinity ration was considered negligible due to the large background Ca^{2+} concentrations in seawater (~10.5 mmol kg^{-1} at a salinity of 35; Gazeau et al., 2015). The combined uncertainty for each computed carbonate chemistry properties is estimated to be ±5 µmol kg^{-1} for DIC, ± 0.005 for pH_T, and ±0.05 for saturation state of $CaCO_3$ minerals (following the procedures proposed by Orr et al., 2018).

2.5.2. Instantaneous diffusive air-water CO_2 fluxes

Instantaneous diffusive fluxes of CO_2 at the air-water interface were calculated according to the following equation:

$$FCO_2 = k_{CO2,T} * s * \Delta fCO_2 \tag{5}$$

Where FCO_2 is the diffusive flux of CO_2, $k_{CO2,T}$ is the gas transfer velocity of CO_2 at a given temperature (T), s is the solubility coefficient of CO_2 calculated from *in situ* SST and SSS (Weiss, 1974), and the ΔCO_2 is the difference between the fCO_2 measured in water (fCO_2sw) and the fCO_2measured in the atmosphere (fCO_2air). The gas transfer velocity of CO_2 $k_{CO2,T}$ was computed as follows (Jähne et al., 1987):

$$k_{CO2,T} = k_{600} * (600/Sc_{CO2,\ T})^n \tag{6}$$

where k_{600} is the gas transfer velocity normalized to a Schmidt number of 600 (Sc = 600 for CO_2 at 20°C), $Sc_{CO2,\ T}$ is the Schmidt number of CO_2 at a given temperature (Wanninkhof, 1992), and n is -0.5 inferred from the wind speed (Jähne et al., 1987; Wanninkhof, 1992).

To compute the k_{600} values, we used the parameterization proposed by Wanninkhof (2014):

$$k_{600}(W14) = 0.251 * (U_{10}{}^{\wedge 2}) \tag{7}$$

where k_{600} is the gas transfer velocity normalized to a Schmidt number of 600 expressed in cm h^{-1}, and U_{10} is the wind speed at 10m height in m s^{-1}.

2.6. Statistical analysis

We applied the Shapiro–Wilk test to investigate the normality of the data set. As the data did not follow normal distributions, non-parametric statistics were used. To compare the differences between averages, the Mann–Whitney test was applied, which compares the distributions of unmatched groups. Linear regressions were calculated to analyse the correlations between variables, providing the best-fit slope, the intercept and the goodness of fit (R^2). All statistical analyses were based on α = 0.05. The statistical tests and calculations were performed with the Graph Pad Prism 6 program.

3. Results

Table 1 shows averages, standard deviation, minimum and maximum values of the main parameters measured and calculated in this study. Nearshore region included stations with longitudes >38°26.0' W, whereas the coral reef-dominated waters included the stations with longitude <38°26.0' W. The SST did not present a clear spatial variability ($p > 0.05$; Mann-Whitney test), instead, it was related to the hour of sampling with a typical diurnal pattern, i.e., lower values in the early-morning (minimum = 27.7°C) and higher values at midday-afternoon periods (maximum = 29.3°C) (Fig. 2). The SSS presented a slight spatial variability. Higher values were found in the nearshore region (highest = 36.5), whereas lower values were found in the coral

Table 1
Spatial variability (mean, standard deviation, minimum and maximum values) for the principal physicochemical and seawater carbonate chemistry parameters analysed in this study.

	Nearshore waters N = 9	Coral reef-dominated waters N = 11
SSS [a]	36.1 ± 0.14	36.0 ± 0.10
	36.0 /36.5	35.9 /36.2
SST (°C) [a]	28.2 ± 0.3	28.4 ± 0.3
	28.0 /28.9	28.0 /29.2
O_2 (%sat)	97 ± 5	100 ± 1
	92 /103	98 /102
fCO_2sw (µatm) [a]	458 ± 21	475 ± 28
	419 /530	427 /580
pH_T (Total scale)	8.00 ± 0.007	7.98 ± 0.008
	7.98 /8.01	7.96 /8.00
TA (µmol kg^{-1})	2337 ± 23	2325 ± 19
	2325 /2374	2304 /2364
DIC(µmol kg^{-1})	2017 ± 16	2019 ± 16
	1996 /2050	1995 /2070
HCO_3^-(µmol kg^{-1})	1781 ± 15	1788 ± 15
	1758 /1808	1766 /1814
CO_3^{2-}(µmol kg^{-1})	224 ± 4	217 ± 5
	217 /232	213 /225
Ω_{ara}	3.58 ± 0.05	3.49 ± 0.07
	3.48 /3.69	3.41 /3.61
Chl *a* (µg L^{-1})	0.11 ± 0.09	0.16 ± 0.08
	0.02 /0.29	0.07 /0.33

[a] SSS, SST, and fCO_2sw were measured continuously at frequency of 1 min. For these parameters, the number of samples (N) measured in nearshore and coral reef-dominated waters were, respectively, 670 and 836.

reef-dominated waters (minimum = 35.9). These values of SST and SSS confirm the presence of Tropical Water (TW) in both regions, which is characterized by temperatures higher than 26°C and salinities higher than 36.

Overall, DIC and TA concentrations did not exhibit clear spatial distributions. The average of DIC concentrations was 2017 ± 16 µmol kg^{-1} in the nearshore region, and 2019 ± 16 in the coral reef waters (Mann-Whitney test; $p > 0.05$). For TA, these averages were, respectively, 2337 ± 23 µmol kg^{-1} and 2325 ± 19 µmol kg^{-1} (Mann-Whitney test; $p > 0.05$). However, the two highest values of TA were found in regions further away from the reef, with a maximum concentration of 2376 µmol kg^{-1}. On the contrary, the lowest concentration of TA occurred inside the PRM limits, with a minimum value of 2314 µmol kg^{-1}. The HCO_3^-concentrations followed the tendency of DIC and TA, with no significant spatial variability (Mann-Whitney test; $p > 0.05$), averaging 1782 ± 18 µmol kg^{-1} in the nearshore region, and 1788 ± 15 µmol kg^{-1} in the coral reef waters.

On the other hand, pH_T, CO_3^{2-}, $f$$CO_2$sw and Ω_{ara} showed clear spatial patterns. Coral reef stations showed higher values of $f$$CO_2$sw, and lower values of pH_T, CO_3^{2-}, and Ω_{ara} compared to the nearshore region (Mann-Whitney test; $p < 0.01$). The values of $f$$CO_2$sw showed always over-saturated conditions compared to the $f$$CO_2$air, showing that the region was a permanent source of CO_2 to the atmosphere during all sampled periods (Table 2; Figs. 2 and 3). The $f$$CO_2$sw did not present significant relationship with SST (Fig. 2) and SSS. The average of $f$$CO_2$sw values in the nearshore region was 455 ± 21µatm, whereas in the coral reef this average was 475 ± 28 µatm. The maximal measured $f$$CO_2$sw was 580 µatm found close to the PRM limits (Fig. 3). For pH_T, CO_3^{2-}, and Ω_{ara}, the averages in the nearshore region were, respectively, 8.00 ± 0.008, 223 ± 4 and 3.59 ± 0.07. For the coral reef-dominated waters these averages were, respectively, 7.97 ± 0.007, 217 ± 4, and 3.48 ± 0.06. The minimal values of pH_T, $CO_3^{2-}$and Ω_{ara} were 7.97, 213, and 3.41, respectively, found close to the PRM boundaries. The concentrations of Chl *a* were low for all sampled areas, indicating oligotrophic conditions. The maximal concentration was 0.33 µg L^{-1} found inside the boundaries of the PRM.

The calculated instantaneous fluxes of CO_2 at the air-water interface and ancillary parameters used for fluxes calculations are showed in the Table 2. The wind speed presented averaged values of 6.9 ± 1.6 m s^{-1} and 7.7 ± 1.5 m s^{-1} in the nearshore and coral reef-dominated waters, respectively. The calculated gas transfer velocities using the parameterization of Wanninkhof (2014) followed the tendency of wind velocity, with slightly higher values in the region of coral reefs influence (16.1 ± 8.1 cm h^{-1}) than nearshore region (13.1 ± 7.0 cm h^{-1}). As exposed above, the $f$$CO_2$sw were always higher than $f$$CO_2$air. The values of $f$$CO_2$air were almost constant, showing values of ~406 µtam. The region inside the PRM and adjacent localities exhibited the highest emissions of CO_2 reflecting the higher $f$$CO_2$sw values, averaging 8.4 ± 6.5 mmolC m^{-2} d^{-1} (Mann-Whitney test; $p < 0.001$). The nearshore region emitted about 5.0 ± 3.9 mmolC m^{-2} d^{-1}.

Table 2
Mean (±standard deviations), minimum and maximum values of the wind velocity, gas transfer velocity (k_{600}), fugacity of CO_2 in surface water ($f$$CO_2$sws) and in the atmosphere ($f$$CO_2$air), and calculated instantaneous air-water CO_2 Fluxes (FCO_2), separated in nearshore and coral reef-dominated waters.

	Wind Velocity (m s^{-1})	k_{600} (cm s^{-1})	$f$$CO_2$air (µatm)	$f$$CO_2$sw (µatm)	Instantaneous FCO_2 (mmolC m^{-2} d^{-1})
Nearshore waters N = 670	6.9 ± 1.6 2.9 12.0	13.1 ± 7.1 2.1 36.1	406 ± 3 403 408	458 ± 21 419 520	5.0 ± 3.9 0.35 25.7
Coral reef-dominated waters N = 836	7.7 ± 1.5 3.5 12.8	16.1 ± 8.1 3.0 41.2	405 ± 3 403 407	475 ± 28 427 580	8.4 ± 6.5 0.52 46.6

4. Discussion

4.1. Factors controlling seawater carbonate chemistry

This study presented direct underway $f$$CO_2$sw, $f$$CO_2$air measurements and calculated air-sea CO_2 fluxes in a region of the Brazilian Northeast continental shelf dominated by warm-water coral reefs. This study also presented the results of the main carbonate chemistry parameters, including TA, DIC, HCO_3^-, CO_3^{2-} and Ω_{ara}. To our best knowledge, this is the first report of these parameters in an area of coral reefs coverage in the entire South Atlantic Ocean. This portion of the continental shelf exhibited spatial variability in the distributions of carbonate chemistry parameters, especially for $f$$CO_2$sw, pH, CO_3^{2-} and Ω_{ara}. Overall, the coral-dominated reef in waters presented higher values of $f$$CO_2$sw when compared to nearshore waters. These high $f$$CO_2$sw in the

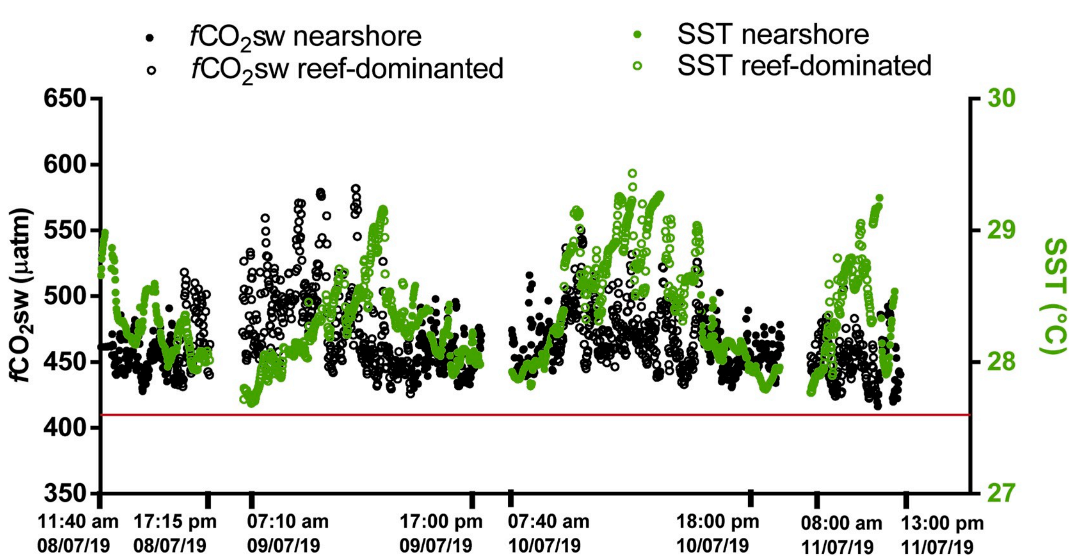

Fig. 2. Continuous underway measurements of $f$$CO_2$sw (y-left axis) and SST (y-right axis) plotted against time and day of sampling. The red line represents the averaged values of atmospheric CO_2 fugacity ($f$$CO_2$air). Filled circles represent nearshore waters. Open circles represent coral reef-dominated waters. (For interpretation of the references to colour in this figure legend, the reader is referred to the Web version of this article.)

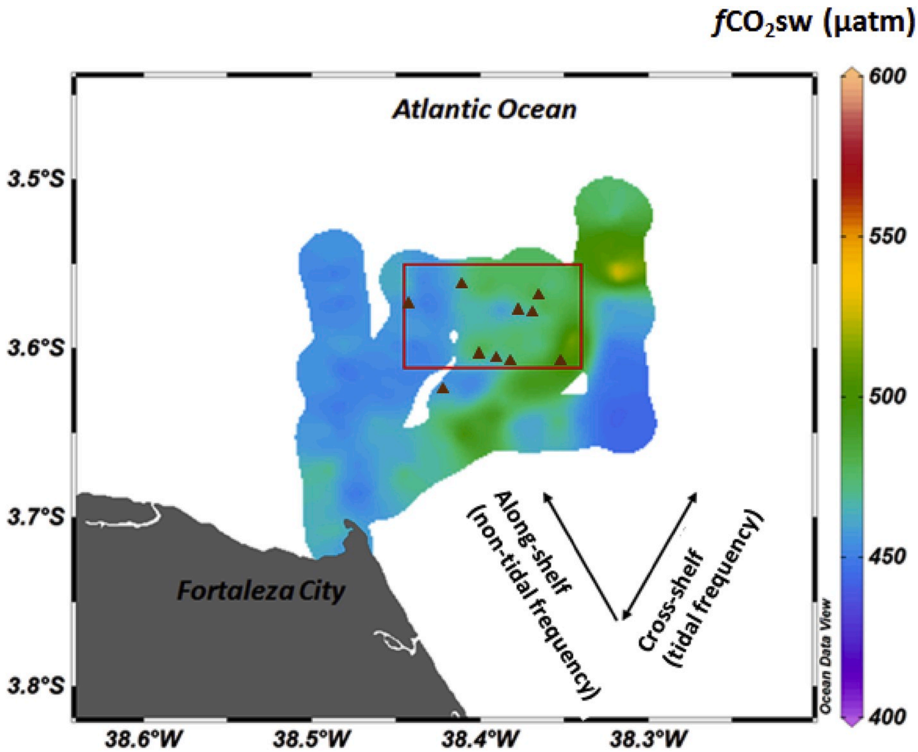

Fig. 3. Composite map showing the spatial distributions of the fCO_2sw values in surface waters of the *Marine State Park of Pedra da Risca do Meio* (PRM) and nearshore localities. The red rectangle represents the limits of the PRM. The blue triangles represents the main linear rock formations associated with coral reefs occurrence. The black arrows represents the along-shore and cross-shore directions of currents. (For interpretation of the references to colour in this figure legend, the reader is referred to the Web version of this article.)

coral reefs are attributed to the process of net $CaCO_3$ precipitation (or Net Community Calcification, NCC), as this process evolves the production of CO_2, and consumption of TA and DIC in a ratio of 2:1 (equation (1)), i.e., for every mole of produced $CaCO_3$ (calcification), TA decreases by 2 mol and DIC decreases by 1 mol (Albright et al., 2013). Other processes could also alter the TA:DIC relationship in coral reefs. The Net Community Production (NCP) refers to the balance between gross primary production and community respiration, which take up or release 1 mol of DIC for every mole of organic carbon, with an almost negligible alteration in TA. The slope of TA:DIC approaches 0 in ecosystems dominated by NCP; while the slope approaches 2 in ecosystems dominated by NCC (Cyronak et al., 2018). Despite the fact that nearshore waters presented lower values of fCO_2sw than coral-reef dominated waters, it is possible to occur water mixing between these two areas depending on the along-shore and cross-shore directions of currents (Fig. 3). This could explain some high values of fCO_2sw in nearshore waters (max. 520 µatm) and the poor relationship between fCO_2sw and SST during the sampled period (Fig. 2).

Fig. 4 presents the relationship between salinity-normalized TA (nTA) and salinity-normalized DIC (nDIC) for all the sampled stations, separated in nearshore and coral reef locations. The station used for salinity-normalization of TA and DIC was far from the PRM boundary, and exhibited the highest value of nTA. Overall, coral reefs showed depletion of TA relative to adjacent open ocean waters (Bates et al., 2001; Cyronak et al., 2018). Fig. 4 shows that the slope of the nTA-nDIC linear regression for the coral-dominated reef area is 1.26, with data distribution approaching the vector calculated for $CaCO_3$ precipitation, whereas for nearshore locations (non-reef dominated) the slope is 1.05. Values higher or lower than 1 indicates that the parameters of the seawater carbonate chemistry can changes considerably because the isolines of pH are crossed (Cyronak et al., 2018). These results reinforce the occurrence of $CaCO_3$ precipitation in the coral-dominated reef in waters, which presented the highest values of fCO_2sw and lowest values of pH, CO_3^{2-} and Ω_{ara}. The $CaCO_3$ precipitation decreases the concentration of TA and DIC, whereas dissolution increases. This can explain the highest concentrations of TA in nearshore locations, where

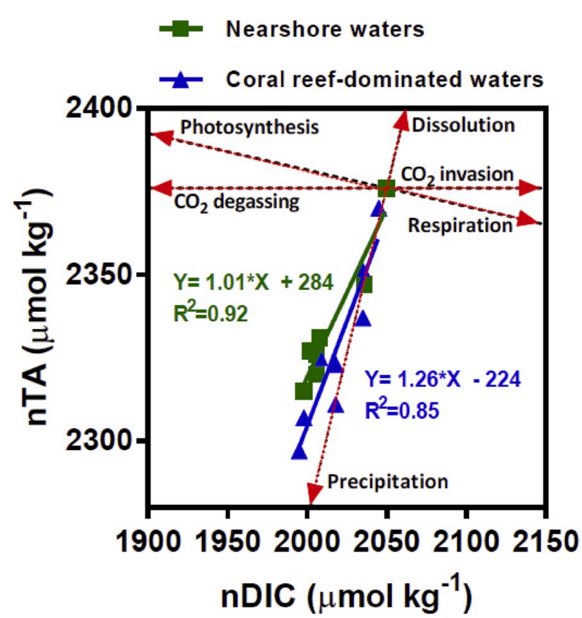

Fig. 4. Relationship between seawater salinity-normalized TA (nTA) and salinity-normalized DIC (nDIC) for all discrete data. TA and DIC were normalized to an average salinity of 36.1 according to Friis et al. (2003). The red arrows represent the slopes of the main processes affecting this relationship. (For interpretation of the references to colour in this figure legend, the reader is referred to the Web version of this article.)

presumably the calcification does not occur, corroborating previous studies (Bates et al., 2001; Andersson et al., 2013; Muellenhner et al., 2016; Cyronak et al., 2018). During all sampled period, the waters were well oxygenated, indicating that $CaCO_3$ dissolution and the production of TA by hypoxic/anoxic processes are very unlikely to occur.

The DIC variability is not only driven by calcification and dissolution of $CaCO_3$, but also by the NCP, in addition to the influx and efflux of CO_2

at the air-water interface (Fig. 4). The processes of photosynthesis and degassing of CO_2 lead to a decrease of DIC concentrations because they remove CO_2 from the water. However, primary production seems to be weak in the region under influence of coral reefs due to the prevalence of oversaturated conditions of CO_2 with respect to the equilibrium with atmosphere, and the slope of nTA-nDIC > 1. The higher Chl *a* content (over 45%) in coral reefs compared to nearshore waters (Table 1) would imply higher CO_2 consumption and low values of fCO_2sw, which did not occur. This reinforces the dominant role of inorganic metabolism (NCC) instead of organic metabolism (NCP) as responsible for the higher *f*CO_2sw values observed in the coral reef region. Nevertheless, it is important to point out that the sampling was conducted only during daytime due to logistical imitations. Calcification in the light is significantly higher than calcification in the dark, while photosynthesis does not occurs in the dark (Gattuso et al., 1999). The decreasing calcification rates during nighttime tend to decreases the production of CO_2. On the other hand, the absence of primary production during nighttime tends to increases the production of CO_2 by respiratory processes. Studies have showed that the community gross primary production are almost equivalent to the community respiration in coral reefs (Gattuso et al., 1999). This implies that the net production of CO_2 by organic metabolism (NCP) is close to zero, and the release of CO_2 is most driven by $CaCO_3$ precipitation (NCC) (Ware et al., 1992; Gattuso et al., 1993, 1999; Frankignoulle et al., 1996). We could not find significant drawdown of CO_2 values in different hours along the day (e.g., midday, early morning) supposedly due to low levels of photosynthesis in these oligotrophic waters. However, these processes require further investigations at diel time scales.

Overall, studies conducted in other coral reef environments have shown that slopes of nTA/nDIC >1 are typical of coral sampled with a significant spatial component (>10 km^2), whereas values of nTA/nDIC < 1 are typical in corals sampled at one position (Eulerian approach) (Cyronal et al., 2018). The values in PRM are very close to that found in the coral reefs of FL Keys (North Atlantic), Bermuda (North Atlantic) and Majuro (Indo Pacific) (Andersson et al., 2013; Muellenhner et al., 2016; Cyronal et al., 2018). When the studies encompass large spatial scales, the signal on the carbonate chemistry is integrated of several coral reef habitats, rather than specific ones (Cyronak et al., 2018). Larger spatial scales tend to present NCP close to zero (Gattuso et al., 1999). On the other hand, studies with high temporal frequency tend to integrate the organic metabolic pulse reflecting the dominance of primary production during the day time (decreasing DIC and increasing pH), and respiration during night-time (increasing DIC and decreasing pH) (Gattuso et al., 1993; Frankignoulle et al., 1996; Anthony et al., 2011). We did not find significant relationship between the levels of CO_2 and dissolved oxygen in seawater, corroborating the minor influence of photosynthesis and respiration. The averaged values of *f*CO_2sw, CO_3^{2-} and Ω_{ara} found in the PRM coral reefs were very similar to that found in other coral reefs, including studies in the Pacific, Indian, and North Atlantic Oceans (Suzuki et al., 1995; Silverman et al., 2007;Shamberger et al., 2011 ; Albright et al., 2013; Cyronak et al., 2018). However, it is remarkable that our ranges of values are lower than most studies, which reflects our sampling design turned to spatial investigation (sampling across large spatial scale; >10km^2).

The biogeochemical process of net $CaCO_3$ precipitation could locally exacerbate the ocean acidification (Anthony et al., 2011; Kelypas et al., 2011; Andersson et al., 2013; Cyronak et al., 2014). It is important to point out that the thermodynamic predicts the dissolution of $CaCO_3$ when the value of Ω_{ara} decreases to value lower than 1. However, a recent study showed that coral reefs could reach net dissolution at Ω_{ara} of around 2.3 with 100% living coral cover, and at $\Omega_{ara} > 3.5$ with 30% of living coral cover (Kline et al., 2019). This threshold between net dissolution and calcification is affected by the proportion of living corals on a reef, suggesting that exists a relationship between ocean acidification and bleaching vulnerability (Kline et al., 2019). Coral bleaching occurrences are becoming more severe and frequent in space and time, resulting in mass coral mortality (Hughes et al., 2017). For instance, a recent study has reported a mass bleaching event in the scleractinian coral (hard corals) *Siderastrea stellata* Verrill in the PRM colonies (Soares et al., 2019). The authors attributed this coral bleaching to anomalies in SST (28.5–29.5 °C; from 1 to 1.7 °C above the average), in addition to the low turbidity, and weak winds. The IPCC predicts higher mean SST and marine heatwaves days in the next decades (IPCC, 2019). This situation can be critical in the corals of PRM because dead corals reach net dissolution at a $\Omega_{ara} = 3.5$ (Kline et al., 2019), which is close to the saturation state we found in the present study. The predicted increase and expansion of bleaching events as the result of global warming and marine heatwaves may cause deleterious effects on the corals of PRM and could arrive early than thought because mortality of corals can accelerate the skeleton dissolution. In short, the corals of the PRM can change from net calcification to net dissolution in a near future considering the increasing levels of atmospheric CO_2 and global warming, with amplification of coral bleaching events. In other scenario, considering the PRM with 100% of living corals, the net dissolution is predicted until the end of this century (considering the actual growth rates of atmospheric CO_2 concentrations). The negative effects of global warming, increase marine heatwaves and ocean acidification needs urgent investigation.

4.2. *f*CO_2*sw in coral reef-dominated waters and the regional context*

The *f*CO_2w variability in the North and Northeast continental shelf of Brazil is poorly investigated. The few studies available in these low latitude regions in the South Atlantic showed that the *f*CO_2sw is controlled mainly by biological activities in the North portion due to the influence of the Amazon River Plume (Lefèvre et al., 2017a), whereas the thermodynamic is predominant in the Northeast portion (Araujo et al., 2019). However, this generalization needs to be done carefully because the North and Northeast continental shelves are themselves heterogeneous. A recent study showed important *f*CO_2sw variability considering the along-shore direction in the Northeast coast (Carvalho et al., 2017). This study revealed that the CO_2 variability at the westernmost part of the Northeast coast is mainly driven by biological activities (despite the oligotrophic conditions), whereas the easternmost portion was mainly controlled by temperature and salinity. Another study conducted in a low latitude region with cross-shelf transect off the coast of Maranhão State (North Brazil) also showed marked heterogeneity, with highest values of *f*CO_2sw observed close to the land and attributed to the inputs of organic and inorganic carbon from terrestrial sources (Lefèvre et al., 2017b). Moreover, we address here that the presence of carbonate coral reefs in the continental shelf of Brazil could also alter in a significant way the variability of *f*CO_2sw and the carbonate chemistry in surface waters. The Northeast coast of Brazil presents an extensive portion of the continental shelf covered by modern and relict sediments in the form of bioclastic-siliciclastic sediments associated with occurrence of coral reefs, especially on the inner shelf, with some patches attached to the coast and others covering large distances offshore, generally oriented parallel to the coast with depths between 5 and 10 m (Knoppers et al., 1999; Leão et al., 2016; Morais et al., 2019). In addition, it has been recently mapped an extensive Mesophotic Coral Ecosystem ($\sim$9500 km^2) between Brazil and the Caribbean (the Great Amazon Reef System; Moura et al., 2016; Mahiques et al., 2019), with potential implications for seawater carbonate chemistry dynamics and carbon budget calculations.

We compared our results of *f*CO_2sw variability with the study of Carvalho et al. (2017), which sampled a further offshore region along the South Equatorial Atlantic Ocean (Fig. 5). Both studies presented SST-SSS diagrams consistent with the presence of tropical waters (Dias et al., 2013). Considering the *in situ* SST conditions, the values of *f*CO_2sw averaged 465 ± 25 µatm in the coral reef-dominated waters, whereas the offshore region exhibited average of 384 ± 7 µatm (Fig. 5a,c) with a statistical significance (Mann-Whitney test; $p < 0.001$). Comparing these

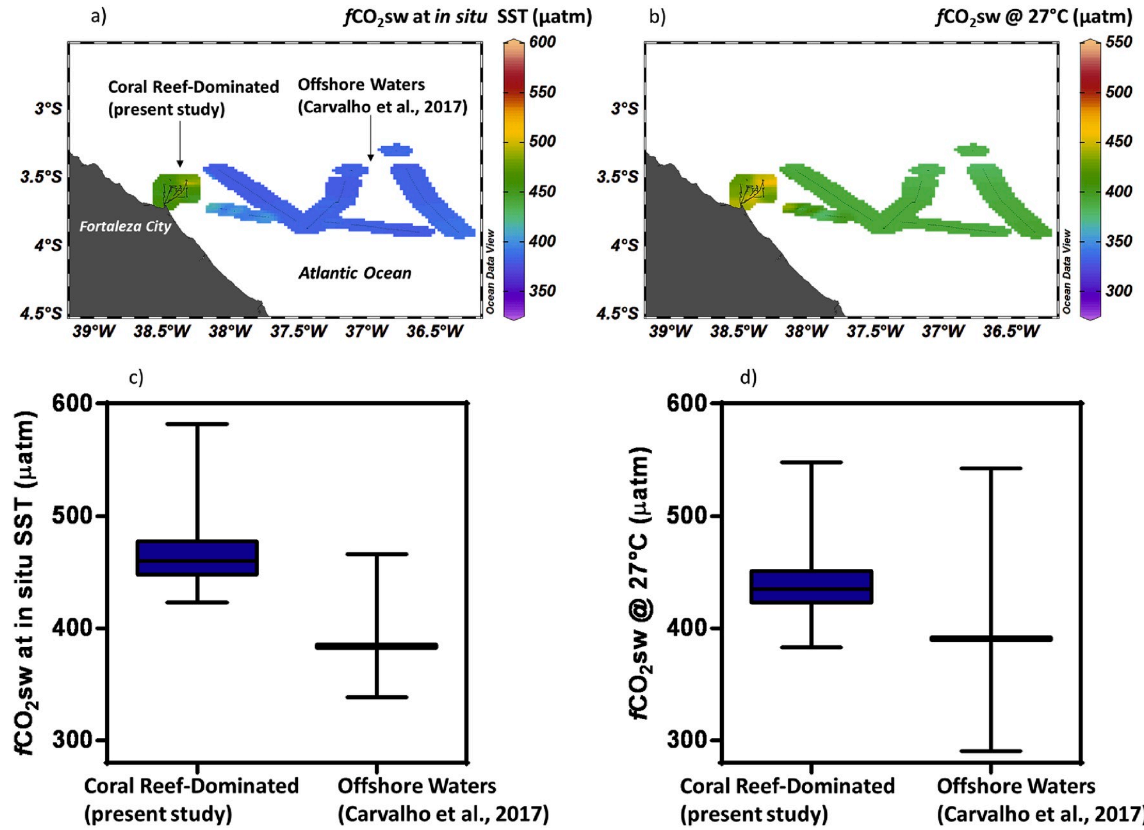

Fig. 5. Comparison between the fCO_2sw spatial variability in the coral reef-dominated waters (present study) and offshore waters with data taken from Carvalho et al. (2017); a) spatial distributions of fCO_2sw at *in situ* SST; b) spatial distributions of fCO_2sw normalized to a temperature of 27 °C (fCO_2sw @27); c) Box plots of fCO_2sw values at *in situ* SST presenting the median and ranges; d) Box plots of fCO_2sw values normalized to a temperature of 27 °C (fCO_2sw @ 27) presenting the median and ranges. Note the different scales in the maps a) and b).

results, it is clear that the coral reef-dominated waters presented higher averages and standard deviations of fCO_2sw values. We applied the procedure of Takahashi et al. (1993) to remove the thermal effect on the fCO_2sw variability by normalizing the fCO_2sw at a constant SST of 27 °C (fCO_2sw at 27°C). After applying this procedure, the difference between averages of these regions decreased, with coral reef region averaging 439 ± 24 µatm and offshore waters averaging 390 ± 13 µatm, however, this condition remains significant at about 50 µatm (Fig. 5b,d). However, the maximum values of fCO_2sw are on the same order of magnitude, suggesting that the study of Carvalho et al. (2017) potentially include some regions under influence of coral reefs. The comparison of temperature-normalized fCO_2sw between these two localities corroborates the high influence of biological effect ($CaCO_3$ precipitation) in waters dominated by coral reefs, showing heterogeneity in the cross-shelf and along-shelf directions. This study corroborates previous findings in other coral-reef ecosystems, in which seawater chemistry on the reef showed higher values and higher variability of fCO_2sw than the adjacent offshore waters (Suzuki and Kawahata, 2003; Albright et al., 2015).

The fCO_2sw variability in the studied region seemed to be also induced by the current direction and water transport. The tidal variability potentially drives the spatial and short-term temporal variabilities of fCO_2sw distributions. Indeed, water circulation is one of the most important drivers of carbon fluxes in coral reefs (Nakamori et al., 1992; Frankignoulle et al., 1996). Some high values of fCO_2sw found in the NNE position of the sampled area (Fig. 3) are consistent with the influence of cross-shelf directional transport (transverse component) during ebb tide (Dias et al., 2018). The net water transport in the continental shelf of Ceará State presents a net NW direction, however, the bathymetry, tidal and subtidal currents, wind velocity and direction can cause considerable deviations from this pattern, even during periods of wind and current reversal (Dias et al., 2018). The seawater carbonate chemistry will incorporates the reef metabolism when the water mass is being transported along the coral reef with the highest signal being incorporated in downstream habitats (Frankignoulle et al., 1996; Anthony et al., 2011). In this way, regions located front and back the coral reef (relative to the direction of the water flow) will present differences as the results of the coral-reef signals (Gattuso et al., 1993; Frankignoule et al., 1996). For the PRM, this situation is even more critical due to the relative high depths where the corals are positioned (~ 24 m depth; Soares et al., 2019). However, even taking account these relative greater depths, the influence of reef-metabolism was evident in surface waters taking account the highest values of surface fCO_2sw in the regions under influence and/or close to the PRM limits. The water column in the region is well-mixed (Dias et al., 2013; Teixeira and Machado, 2013), and the fCO_2sw distributions in the surface waters reflect these complex configurations related to the geographical position of the coral reef communities, water depths, and current direction at the moment of sampling.

4.3. Air-sea CO_2 fluxes and implications

The results of air-sea CO_2 fluxes and parameters used for calculations are presented in Table 2. The sampling campaign was conducted in July-2019, which is a dry period characterized by high energy of winds, with averages of wind velocity exceeding 7 m s^{-1}. The gas transfer velocities presented high values reflecting the high energy of the trade winds. These results are consistent with a previous study in the region (Carvalho et al., 2017). The trade winds in the region are generated from the high-pressure South Atlantic cell and move the Inter-Tropical

Convergence Zone (ITCZ) to northeastern Brazil, with higher velocities during dry period (June to December) (Dias et al., 2013). The Tropical Atlantic Ocean is normally characterized as a net source of CO_2 to the atmosphere (Goyet et al., 1998; Lefèvre et al., 2013). Our study corroborates this emitter behavior, however with stronger intensity. The waters of the PRM and adjacent localities always presented oversaturated conditions with respect the atmosphere CO_2 concentrations, with CO_2 emissions averaging 8.4 ± 6.5 mmolC m^{-2} d^{-1} in the coral reef-dominated waters, and nearshore regions emitting on the order of 5.0 ± 3.9 mmolC m^{-2} d^{-1}. Overall, previous studies in the western Tropical Atlantic Ocean showed different results and lower CO_2 emissions. The averaged emissions by the offshore waters of the North and Northeast coast of Brazil were estimated at about 0.3 ± 1.7 mmolC m^{-2} d^{-1}, with ranges from -1.2 to 2.0 mmolC m^{-2} d^{-1} (Araujo et al., 2019). The authors attributed the sink behavior (negative values) to the influence of the high productivity of the Amazon River Plume, and the source behavior driven mainly by SST variability in the offshore regions (4°S to 12°S). Other study conducted along the Northeast coast of Brazil calculated instantaneous fluxes ranging from 0.89 to 14.62 mmolC $m^{-2}d^{-1}$, with higher emissions associated to the thermal effect (eastern portion), and lower emissions associate to the increase of biological activities and CO_2 uptake (western portion) (Carvalho et al., 2017). Considering the cross-shelf direction, a study conducted in the coast of Maranhão (North Brazil) showed annual mean flux of 1.81 ± 0.84 mmolC m^{-2} d^{-1} in the continental shelf, and annual mean emissions of 2.32 ± 1.09 mmolC m^{-2} d^{-1} for further offshore waters (Lefèvre et al., 2017b). The authors found higher fCO_2sw values close to the land than offshore waters, however, the calculated fluxes did not reflect this gradient because the wind velocity were stronger in the open ocean. In short, comparing our results with those found in these other regions of the North and Northeastern continental shelf of Brazil, it is clear that the presence of coral reefs can alter regionally the magnitude of CO_2 emissions, particularly in shallow waters.

We also compared our calculated emissions of CO_2 with other coral reef environments (Table 3). The availability of studies investigating the emissions of CO_2 by coral-dominated reef in waters is still scarce. In general, all studies quantifying the CO_2 exchanges at the air-sea interface showed a source behavior in marine ecosystems dominated by coral reefs (Frankignoulle and Gattuso, 1994; Gattuso et al., 1999; Kawahata et al., 1997; Lønborg et al., 2019). This is the result of the changes of seawater CO_2 system during calcification, which removes CO_3^{2-} or HCO_3^- and releases CO_2 in the water (Frankignoulle and Gattuso, 1994). The fluxes calculated for the PRM coral reefs compare well with emissions calculated in the Moorea Coral Reef (French Polynesia) and Yong Reef (Australian Great Barrier Reef) (1.8 to 5.1 mmolC m^{-2} d^{-1}; Gattuso et al., 1993; Frankignoulle et al., 1996); Shiraho Reef (Japan) (12.0 mmolC m^{-2} d^{-1}; Nakamori et al., 1992); Hog Reef Flat (Bermuda) (3.3 mmol C m^{-2} d^{-1}; Bates et al., 2001); Tropical Coral Reef Lagoon in Kaneohe Bay (Hawaii) (3.9 to 8.9 mmolC m^{-2} d^{-1}; Fagan and Mackenzie, 2007; Ho et al., 2018), in the Yongle Atoll (South China Sea (SCS))(3.2 mmolC m^{-2} d^{-1}; Yan et al., 2018), and in the Great Barrier Reef (-6.19 to 12.17 mmolC m^{-2} d^{-1}; Lønborg et al., 2019). An overall characteristic is that the observed averages and ranges of air-sea CO_2 fluxes are greater in coral reef habitats than outside the reef influence, reflecting the most active biological activities inside the reefs under stronger influences of organic and inorganic metabolic pulses. Many studies incorporated the diurnal variability on the investigations of carbonate system in coral reefs, with estimations of NCP and NCC. Overall, the NCP presents an almost equilibrium between the rates of primary production and respiration of community, with an almost negligible influence on the air-sea CO_2 exchanges (Gattuso et al., 1999). This suggests that the net calcification is higher relative to net organic production in most reef flats causing CO_2 evasion to the atmosphere (Gattuso et al., 1999). The release of CO_2 during calcification depends on the physicochemical properties of seawater, including the values of fCO_2sw (Frankignoulle and Gattuso, 1994). This means that low values of fCO_2sw results in lower changes of seawater carbonate chemistry compared to high values of fCO_2sw. These accentuated changes in seawater carbonate chemistry are associated to the changes in seawater buffering capacity under a scenario of high CO_2 concentrations, and could provide a positive feedback to the global warming (Frankignoulle and Gattuso, 1994) assuming an equilibrium between the CO_2 concentrations in the oceans and atmosphere.

Table 3
A chronologic compiled data of pCO_2sw or fCO_2sw values, and air-sea CO_2 fluxes with ranges and average values (in parenthesis) documented in coral reefs worldwide. The compiled data include only studies that calculated air-sea CO_2 exchanges.

Ecosystem	fCO_2sw or pCO_2sw [a] (μatm)	Air-water CO_2 fluxes (mmol m^{-2} d^{-1})	Reference
More Reef – French Polynesia	240 to 400	−2.1 to 6.5	Gattuso et al. (1993)
Yong Reef – Australian Great Barrier Reef	250 to 700	−21.6 to 43.2	Frankignoulle et al. (1996)
Shiraho Reef - Japan	NA	(12.0)	Nakamori et al. (1992)
Hog Reef Flat – Bermuda	340 to 470	−0.6 to 29.0 (3.3)	Bates et al. (2001)
Coral Reef Lagoon Kaneohe Bay – Hawaii	386 to 755	3.8 to 8.9	Fagan and Mackenzie (2007); Ho et al. (2018)
Yongle Atoll Lagoon – South China Sea	258 to 748	(3.2)	Yan et al. (2018)
Great Barrier Reef – Australia	227 to 633 (404)	−6.19 to 12.17 (1.44)	Lønborg et al. (2019)
Pedra da Risca do Meio Coral Reef	427 to 581 (475)	0.4 to 12.8 (8.4)	This study

NA = not available.
[a] Data are presented in fCO_2sw or pCO_2sw.

5. Conclusions

The results showed that seawater carbonate chemistry is significantly altered by biogeochemical processes occurring in the coral reef-dominated waters compared to nearshore and offshore localities in the western Atlantic Ocean. In general, coral reef-dominated waters of the PRM presented higher values of fCO_2sw, and lower values of pH_T, CO_3^{2-}, and Ω_{ara} compared to nearshore and offshore waters. These differences were attributed to the process of $CaCO_3$ precipitation occurring in coral reefs as indicated by the relationship between nTA and nDIC showing a slope higher than 1. This evidences that the spatial variability of carbonate chemistry dynamics are driven by the inorganic metabolic pulse (precipitation of $CaCO_3$), which seems predominant over the organic metabolic pulse (organic carbon production and respiration). These lower values of pH_T, CO_3^{2-}, and Ω_{ara} at the region most influenced by coral reefs corroborate previous findings showing that coral reef communities could compound ocean acidification effects with associate changes in seawater carbonate chemistry (Anthony et al., 2011). The vulnerability of the corals face to ocean acidification can be even more critical taking account the recent documented bleaching events in the study area associated to positive anomalies in SST.

The high values of fCO_2sw in the coral-dominated reef in waters reflect in higher CO_2 emissions compared to nearshore and offshore waters. To our best knowledge, this is the first study showing influence of coral reefs on the air-sea CO_2 exchanges in the entire South Atlantic Ocean. Brazilian coral reefs comprises the largest area of reefs in the SW Atlantic Ocean, with reefs spreading over more than 3,000 km alongshore the Brazilian Coast (Leão et al., 2016), including the recent mapped Great Amazon Reef System (Moura et al., 2016; Mahiques et al., 209). This have important implications considering the carbon budget estimates for the North and Northeast continental shelf of Brazil.

Author contributions

Luiz C. Cotovicz Jr.: Conceptualization, Coordination, Execution, Data curation, Formal analysis, Methodology, Writing - original draft. Rozane V. Marins: Conceptualization, Funding acquisition, Project administration, Resources, Supervision, development of fCO_2 measurement system; Writing - review. Raisa Chielle: Execution, Data curation, Methodology, Writing - review. All authors read and approved the final manuscript.

Declaration of competing interest

The authors declare that they have no known competing financial interests or personal relationships that could have appeared to influence the work reported in this paper.

Acknowledgments

This study was financed by the Fundação Cearense de Apoio ao Desenvolvimento Científico e Tecnológico (FUNCAP; Proc. No. INT-00159-00009.01.00/19), and the Programa de Apoio a Núcleos de Excelência (PRONEX; Proc. No. PR2-0101-0052.01.00/2015). We are thankful to the Projeto Áreas Marinhas e Costeiras Protegidas (GEF Mar) and the Secretaria de Meio Ambiente do Estado do Ceará (SEMA-CE) for the opportunity to board the vessel. Luiz C. Cotovicz Jr. thanks the UFC-PRPPG for a visiting professor grant at the Marine Sciences Institute (LABOMAR); Rozane V. Marins thanks the CNPq /Proc. No. 309718/2016-3; and Raiza Chielle thanks the FUNCAP for the Ph.D. grant. Finally, we would like to thank the crew of "Argo Equatorial" oceanographic vessel.

References

Albright, R., Langdon, C., Anthony, K.R.N., 2013. Dynamics of seawater carbonate chemistry, production, and calcification of a coral reef flat, central Great Barrier Reef. Biogeosciences 10, 6747–6758. https://doi.org/10.5194/bg-10-6747-2013.

Albright, R., Benthuysen, J., Cantin, N., Caldeira, K., Anthony, K., 2015. Coral reef metabolism and carbon chemistry dynamics of a coral reef flat. Geophys. Res. Lett. 42, 3980–3988. https://doi.org/10.1002/2015GL063488.

Agostini, S., Harvey, B.P., Wada, S., Kon, K., Milazzo, M., Inaba, K., Hall-Spencer, J.M., 2018. Ocean acidification drives community shifts towards simplified non-calcified habitats in a subtropical−temperate transition zone. Sci. Rep. 8 https://doi.org/10.1038/s41598-018-29251-7.

Andersson, A.J., Yeakel, K.L., Bates, N.R., de Putron, S.J., 2013. Partial offsets in ocean acidification from changing coral reef biogeochemistry. Nat. Clim. Change 4. https://doi.org/10.1038/NCLIMATE2050.

Anthony, K., Kleypas, J., Gattuso, J.-P., 2011. Coral reefs modify their seawater carbon chemistry - implicationsfor impacts of ocean acidification. Global Change Biol. 17, 3655–3666. https://doi.org/10.1111/j.1365-2486.2011.02510.x.

Araujo, M., Noriega, C., Medeiros, C., Lefèvre, N., Ibánhez, J.S.P., Flores Montes, M., Silva, A.C., Santos, M.L., 2019. On the variability in the CO_2 system and water productivity in the western tropical Atlantic off North and Northeast Brazil. J. Mar. Syst. 189, 62–77. https://doi.org/10.1016/j.jmarsys.2018.09.008.

Bates, N., Samuels, L., Merlivat, L., 2001. Biogeochemical and physical factors influencing seawater fCO_2 and air-sea CO_2 exchange on the Bermuda coral reef. Limnol. Oceanogr. 46, 833–846.

Bauer, J.E., Cai, W.-J., Raymond, P.A., Bianchi, T.S., Hopkinson, C.S., Regnier, P.A., 2013. The changing carbon cycle of the coastal ocean. Nature 504, 61–70. https://doi.org/10.1038/nature12857.

Behling, H., Arz, W.H., Pätzold, J., Wefer, G., 2000. Late quaternary vegetational and climate dynamics innortheastern Brazil: inferences from marine core GeoB3104-1. Quat. Sci. Rev. 19, 981–994.

Borges, A., 2005. Do we have enough pieces of the jigsaw to integrate CO_2 fluxes in the coastal ocean? Estuaries 28, 3–27. https://doi.org/10.1007/BF02732750.

Borges, A.V., Delille, B., Frankignoulle, M., 2005. Budgeting sinks and sources of CO_2 in the coastal ocean: diversity of ecosystems counts. Geophys. Res. Lett. 32, L14601. https://doi.org/10.1029/2005GL023053.

Cai, W.-J., 2011. Estuarine and coastal ocean carbon paradox: CO_2 sinks or sites of terrestrial carbon incineration. Annu. Rev. Mar. Sci. 3, 123–145. https://doi.org/10.1146/annurev-marine-120709-142723.

Carvalho, A.C.O., Marins, R.V., Dias, F.J.S., Rezende, C.E., Lefèvre, N., Cavalcante, M.S., Eschrique, S.A., 2017. Air-sea CO_2 fluxes for the Brazilian northeast continental shelf in a climatic transition region. J. Mar. Syst. 173, 70–80. https://doi.org/10.1016/j.jmarsys.2017.04.009.

Chen, C.-T.A., Huang, T.-H., Chen, Y.-C., Bai, Y., He, X., Kang, Y., 2013. Air–sea exchanges of CO_2 in the world's coastal seas. Biogeosciences 10, 6509–6544. https://doi.org/10.5194/bg-10-6509-2013.

Couce, E., Ridgwell, A., Hendy, E.J., 2013. Future habitat suitability for coral reef ecosystems under global warming and ocean acidification. Global Change Biol. 19, 3592–3606. https://doi.org/10.1111/gcb.12335.

Cyronak, T., Santos, I.R., Erler, D.V., Maher, D.T., Eyre, B.D., 2014. Drivers of pCO_2 variability in two contrasting coral reef lagoons: the influence of submarine groundwater discharge. Global Biogeochem. Cycles 28, 398–414. https://doi.org/10.1002/2013GB004598.

Cyronak, T., Andersson, A.J., Langdon, C., Albright, R., Bates, N.R., Caldeira, K., Carlton, R., Corredor, J.E., Dunbar, R.B., Enochs, I., Erez, J., Eyre, B.D., Gattuso, J.P., Gledhill, D., Kayanne, H., Kline, D.I., Koweek, D.A., Lantz, C., Lazar, B., Manzello, D., McMahon, A., Meléndez, M., Page, H.N., Santos, I.R., Schulz, K.G., Shaw, E., Silverman, J., Suzuki, A., Teneva, L., Watanabe, A., Yamamoto, S., 2018. Taking the metabolic pulse of the world's coral reefs. PloS One 13. https://doi.org/10.1371/journal.pone.0190872.

Dias, F.J.S., Castro, B.M., Lacerda, L.D., 2013. Continental shelf water masses off the jaguaribe river (4S), northeastern Brazil. Continent. Shelf Res. 66, 123–135. https://doi.org/10.1016/j.csr.2013.06.005.

Dias, F.J.S., Castro, B.M., Lacerda, L.D., 2018. Tidal and low-frequency currents off the Jaguaribe River estuary (4° S, 37° 4′ W), northeastern Brazil. Ocean Dynam. 68, 967–985. https://doi.org/10.1007/s10236-018-1172-6.

Dickson, A.G., Millero, F.J., 1987. A comparison of the equilibrium constants for the dissociation of carbonic acid in seawater media. Deep-Sea Res. 34, 1733–1743. https://doi.org/10.1016/0198-0149(87)90021-5.

Dickson, A.G., 1990. Thermodynamics of the dissociation of boric acid in synthetic seawater from 273.15 to 318.15 K. Deep-Sea Res. I Oceanogr. Res. Pap. 37, 755–766. https://doi.org/10.1016/0198-0149(90)90004-F.

Dickson, A.G., 2010. The carbon dioxide system in seawater: equilibrium chemistry and measurements. In: Riebesell, U., Fabry, V.J., Hansson, L., Gattuso, J.-.P. (Eds.), Guide to Best Practices for Ocean Acidification Research and Data Reporting. Publications Office of the European Union, Luxembourg, pp. 17–40.

Doney, S.C., Fabry, V.J., Feely, R., Kleypas, J.A., 2009. Ocean acidification: the other CO2 problem. Annu. Rev. Mar. Sci. 1, 169–192. https://doi.org/10.1146/annurev.marine.010908.163834.

Fagan, K., Mackenzie, F.T., 2007. Air–sea CO_2 exchange in a subtropical estuarine-coral reef system, Kaneohe Bay, Oahu, Hawaii. Mar. Chem. 106, 174–191.

Feely, R., Sabine, C.L., Lee, K., Berelson, W., Kleypas, J., Fabry, V.J., Millero, F.J., 2004. Impact of anthropogenic CO_2 on the $CaCO_3$ system in the oceans. Science 305, 362–366. https://doi.org/10.1126/science.1097329.

Frankignoulle, M., Gattuso, J.-P., 1994. Marine calcification as a source of carbon dioxide: positive feedback of increasing atmospheric CO_2. Limnol. Oceanogr. 39, 458–462.

Frankignoulle, M., Gattuso, J.-P., Biondo, R., Bourge, I., Copin-Montegut, G., Pichon, M., 1996. Carbon fluxes in coral reef. II. Eulerian study of inorganic carbon dynamic and measurement of air-sea exchange. Mar. Ecol. Prog. Ser. 145, 123–132.

Friis, K., Körtzinger, A., Wallace, D.W.R., 2003. The salinity normalization of marine inorganic carbon chemistry data. Geophys. Res. Lett. 30, 1085. https://doi.org/10.1029/2002GL015898.

Gattuso, J.-P., Pichon, M., Delesalle, B., Frankignoulle, M., 1993. Community metabolism and air-sea CO_2 fluxes in acoral reef ecosystem (Moorea, French Polynesia). Mar. Ecol.: Prog. Ser. 96, 259–267.

Gattuso, J.-P., Frankignoulle, M., Smith, S.V., 1999. Measurement of community metabolism and significance in the coral reef CO_2 source-sink debate. Proc. Natl. Acad. Sci. Unit. States Am. 96, 13017–13022. https://doi.org/10.1073/pnas.96.23.13017.

Gattuso, J.-P., Magnan, A., Billé, R., Cheung, W.W.L., Howes, E.L., Joos, F., Allemand, D., Bopp, L., Cooley, S.R., Eakin, C.M., Hoegh-Guldberg, O., Kelly, R.P., Pörtner, H.-O., Rogers, A.D., Baxter, J.M., Laffoley, D., Osborn, D., Rankovic, A., Rochette, J., Sumaila, U.R., Treyer, S., Turley, C., 2015. Contrasting futures for ocean and society from different anthropogenic CO_2 emissions scenarios. Science 349. https://doi.org/10.1126/science.aac4722.

Gazeau, F., Urbini, L., Cox, T.E., Alliouane, S., Gattuso, J.-P., 2015. Comparison of the alkalinity and calcium anomaly techniques to estimate rates of net calcification. Mar. Ecol. Prog. Ser. 527, 1–12. https://doi.org/10.3354/meps11287.

Goyet, C., Adams, R., Eischeid, G., 1998. Observations of the CO_2 system properties in the tropical Atlantic Ocean. Mar. Chem. 60, 49–61. https://doi.org/10.1016/S0304-4203(97)00081-9.

Gran, G., 1952. Determination of the equivalence point in potentiometric titrations-Part II. Analyst 77, 661–671.

Ho, D.T., De Carlo, E.H., Schlosser, P., 2018. Air-Sea gas exchange and CO_2 fluxes in a tropical coral reef lagoon. J. Geophys. Res. Oceans 123, 8701–8713. https://doi.org/10.1029/2018JC014423.

Hoegh-Guldberg, O., Poloczanska, E.S., Skirving, W., Dove, S., 2017. Coral reef ecosystems under climate change and ocean acidification. Front. Mar. Sci. 4 https://doi.org/10.3389/fmars.2017.00158.

Hughes, T.P., Kerry, J.T., Álvarez-Noriega, M., Álvarez-Romero, J.G., Anderson, K.D., Baird, A.H., Babcock, R.C., Beger, M., Bellwood, D.R., Berkelmans, R., Bridge, T.C., Butler, I.R., Byrne, M., Cantin, N.E., Comeau, S., Connolly, S.R., Cumming, G.S., Dalton, S.J., Diaz-Pulido, G., Eakin, C.M., Figueira, W.F., Gilmour, J.P., Harrison, H. B., Heron, S.F., Hoey, A.S., Hobbs, J.P.A., Hoogenboom, M.O., Kennedy, E.V., Kuo, C.Y., Lough, J.M., Lowe, R.J., Liu, G., McCulloch, M.T., Malcolm, H.A., McWilliam, M.J., Pandolfi, J.M., Pears, R.J., Pratchett, M.S., Schoepf, V., Simpson, T., Skirving, W.J., Sommer, B., Torda, G., Wachenfeld, D.R., Willis, B.L.,

Wilson, S.K., 2017. Global warming and recurrent mass bleaching of corals. Nature 543, 373–377. https://doi.org/10.1038/nature21707.
IPCC, 2013. In: Stocker, T.F., Qin, D., Plattner, G.-K., Tignor, M., Allen, S.K., Boschung, J., Nauels, A., Xia, Y., Bex, V., Midgley, P.M. (Eds.), Climate Change 2013: the Physical Science Basis. Contribution of Working Group I to the Fifth Assessment Report of the Intergovernmental Panel on Climate Change. Cambridge University Press, Cambridge, United Kingdom and New York, NY, USA, p. 1535.
IPCC, 2019. Summary for policymakers. In: Pörtner, H.-O., Roberts, D.C., Masson-Delmotte, V., Zhai, P., Tignor, M., Poloczanska, E., Mintenbeck, K., Nicolai, M., Okem, A., Petzold, J., Rama, B., Weyer, N. (Eds.), IPCC Special Report on the Ocean and Cryosphere in a Changing Climate. In press.
Jähne, B., Munnich, K.O., Bosinger, R., Dutzi, A., Huber, W., Libner, P., 1987. On parameters influencing air-water exchange. J. Geophys. Res. 92, 1937–1949. https://doi.org/10.1029/JC092iC02p01937.
Kawahata, H., Suzuki, A., Goto, K., 1997. Coral reef ecosystems as a source of atmospheric CO_2: evidence from PCO_2 measurements of surface waters. Coral Reefs 16, 261–266. https://doi.org/10.1007/s003380050082.
Kleypas, J.A., Anthony, K.R.N., Gattuso, J.-P., 2011. Coral reefs modify their seawater carbon chemistry - case study from a barrier reef (Moorea, French Polynesia). Global Change Biol. 17, 3667–3678. https://doi.org/10.1111/j.1365-2486.2011.02530.x.
Kline, D.I., Teneva, L., Okamoto, D.K., Schneider, K., Caldeira, K., Miard, T., Chai, A., Marker, M., Dunbar, R.B., Mitchell, B.G., Dove, S., Hoegh-Guldberg, O., 2019. Living coral tissue slows skeletal dissolution related to ocean acidification. Nat. Ecol. Evol. 3, 1438–1444. https://doi.org/10.1038/s41559-019-0988-x.
Knoppers, B.A., Ekau, W., Figueiredo, A.G., 1999. The coast and shelf of east and northeast Brazil and material transport. Geo Mar. Lett. 19, 171–178.
Laruelle, G.G., Cai, W., Hu, X., Gruber, N., Mackenzie, F.T., Regnier, P., 2018. Continental shelves as a variable but increasing global sink for atmospheric carbon dioxide. Nat. Commun. 9, 454. https://doi.org/10.1038/s41467-017-02738-z.
Le Quéré, C., Andrew, R.M., Friedlingstein, P., Sitch, S., Hauck, J., Pongratz, J., Pickers, P.A., Korsbakken, J.I., Peters, G.P., Canadell, J.G., Arneth, A., Arora, V.K., Barbero, L., Bastos, A., Bopp, L., Chevallier, F., Chini, L.P., Ciais, P., Doney, S.C., Gkritzalis, T., Goll, D.S., Harris, I., Haverd, V., Hoffman, F.M., Hoppema, M., Houghton, R.A., Hurtt, G., Ilyina, T., Jain, A.K., Johannessen, T., Jones, C.D., Kato, E., Keeling, R.F., Goldewijk, K.K., Landschützer, P., Lefèvre, N., Lienert, S., Liu, Z., Lombardozzi, D., Metzl, N., Munro, D.R., Nabel, J.E.M.S., Nakaoka, S.-I., Neill, C., Olsen, A., Ono, T., Patra, P., Peregon, A., Peters, W., Peylin, P., Pfeil, B., Pierrot, D., Poulter, B., Rehder, G., Resplandy, L., Robertson, E., Rocher, M., Rödenbeck, C., Schuster, U., Schwinger, J., Séférian, R., Skjelvan, I., Steinhoff, T., Sutton, A., Tans, P.P., Tian, H., Tilbrook, B., Tubiello, F.N., van der Laan-Luijkx, I.T., van der Werf, G.R., Viovy, N., Walker, A.P., Wiltshire, A.J., Wright, R., Zaehle, S., Zheng, B., 2018. Global carbon budget 2018. Earth Syst. Sci. Data 10, 2141–2194. https://doi.org/10.5194/essd-10-2141-2018.
Leão, Z.M.A.N., Kikuchi, R.K.P., Ferreira, B.P., Neves, E.G., Sovierzoski, H.H., Oliveira, M.D.M., Maida, M., Correia, M.D., Johnsson, R., 2016. Brazilian coral reefs in a period of global change: a synthesis. Braz. J. Oceanogr. 64, 97–116. https://doi.org/10.1590/S1679-875920160916064sp2.
Lee, K., Kim, T.W., Byrne, R.H., Millero, F.J., Feely, R.A., Liu, Y.M., 2010. The universal ratio of boron to chlorinity for the North Pacific and North Atlantic oceans. Geochem. Cosmochim. Acta 74, 1801–1811. https://doi.org/10.1016/j.gca.2009.12.027.
Lefèvre, N., Caniaux, G., Janicot, S., Gueye, A., 2013. Increased CO_2 outgassing in february-may 2010 in the tropical atlantic following the 2009 pacific el Niño. J. Geophys. Res. Oceans 118, 1645–1657. https://doi.org/10.1002/jgrc.20107.
Lefèvre, N., Montes, M.F., Gaspar, F.L., Rocha, C., Jiang, S., Araujo, M., Ibanhez, S., 2017a. Net heterotrophy in the Amazon continental shelf changes rapidly to a sink of CO_2 in the outer Amazon Plume. Front. Mar. Sci. 4, 1–16. https://doi.org/10.3389/fmars.2017.00278.
Lefèvre, N., Dias, F.J., Torres, A.R., Noriega, C., Araujo, M., Castro, A.C., Rocha, C., Jiang, S., Ibanhez, S., 2017b. A source of CO_2 to the atmosphere throughout the year in the Maranhense continental shelf (2°30'S, Brazil). Continent. Shelf Res. 141, 38–50. https://doi.org/10.1016/j.csr.2017.05.004.
Lønborg, C., Calleja, M., Fabricius, K., Smith, J., Achterberg, E., 2019. The Great barrier reef: a source of CO2 to the atmosphere. Mar. Chem. 210, 24–33. https://doi.org/10.1016/j.marchem.2019.02.003.
Mahiques, M.M., Siegle, E., Francini-Filho, R.B., Thompson, F.L., de Rezende, C.E., Gomes, J.D., Asp, N.E., 2019. Insights on the evolution of the living Great Amazon reef system, equatorial west atlantic. Sci. Rep. 9 https://doi.org/10.1038/s41598-019-50245-6.
Marques, W., Sial, A.N., Menor, E., Ferreira, V., Frire, G., Lila, E., Souza, R., 2008. Ancient coastlines in the continental shelf of the state of Ceará, northeast Brazil: evidence from sediment chemistry and stable isotopes. Int. Geol. Rev. 50, 1–16. https://doi.org/10.2747/0020-6814.50.4.1.
Mehrbach, C., Cuberson, C.H., Hawley, J.E., Pytkowicz, R.M., 1973. Measurements of the apparent dissociation constants of carbonic acid in seawater at atmospheric pressure. Limnol. Oceanogr. 18, 897–907. https://doi.org/10.4319/lo.1973.18.6.0897.
Millero, F.J., 1979. The thermodynamics of the carbonate system in seawater. Geochem. Cosmochim. Acta 43, 1651–1661.
Morais, J.O., Ximenes Neto, A.R., Pessoa, P.R., Pinheiro, L.S., 2019. Morphological and sedimentary patterns of a semi-arid shelf, Northeast Brazil. Geo Mar. Lett. https://doi.org/10.1007/s00367-019-00587-x.
Morse, J.W., Arvidson, R.S., Lüttge, A., 2007. Calcium carbonate formation and dissolution. Chem. Rev. 107, 342–381. https://doi.org/10.1021/cr050358j.
Moura, R.L., Amado-Filho, G.M., Moraes, F.C., Brasileiro, P.S., Salomon, P.S., Mahiques, M.M., Bastos, A.C., Almeida, M.G., Silva, J.M., Araujo, B.F., Brito, F.P., Rangel, T.P., Oliveira, B.C.V., Bahia, R.G., Paranhos, R.P., Dias, R.J.S., Siegle, E., Figueiredo, A.G., Pereira, R.C., Leal, C.V., Hajdu, E., Asp, N.E., Gregoracci, G.B., Neumann-Leitão, S., Yager, P.L., Francini-Filho, R.B., Fróes, A., Campeão, M., Silva, B.S., Moreira, A.P.B., Oliveira, L., Soares, A.C., Araujo, L., Oliveira, N.L., Teixeira, J.B., Valle, R.A.B., Thompson, C.C., Rezende, C.E., Thompson, F.L., 2016. An extensive reef system at the Amazon River mouth. Sci. Adv. 2, 1–12. https://doi.org/10.1126/sciadv.1501252.
Muehllehner, N., Langdon, C., Venti, A., Kadko, D., 2016. Dynamics of carbonate chemistry, production and calcification of the Florida Reef Tract (2009-2010): evidence for seasonal dissolution. Global Biogeochem. Cycles 30, 661–688. https://doi.org/10.1002/2015GB005327.
Mucci, A., 1983. The solubility of calcite and aragonite in seawater at various salinities, temperatures, and one atmosphere total pressure. Am. J. Sci. 283, 780–799.
Nakamori, T., Suzuki, A., Iryu, Y., 1992. Water circulation and carbon flux on Shiraho coral reef of the Ryukyu Islands. Japan. Cont. Shelf Res. 12, 951–970. https://doi.org/10.1016/0278-4343(92)90054-N.
Orr, J.C., Epitalon, J.-M., Dickson, A., Gattuso, J.-P., 2018. Routine uncertainty propagation for the marine carbon dioxide system. Mar. Chem. 207, 84–107. https://doi.org/10.1016/j.marchem.2018.10.006.
Pierrot, D., Neill, C., Sullivan, K., Castle, R., Wanninkhof, R., Lüger, H., Johannessen, T., Olsen, A., Feely, R.A., Cosca, C.E., 2009. Recommendations for autonomous underway pCO_2 measuring systems and data-reduction routines. Deep-Sea Res. Pt. II 56, 512–522. https://doi.org/10.1016/j.dsr2.2008.12.005.
Robbins, L.L., Hansen, M.E., Kleypas, J.A., Meylan, S.C., 2010. CO_2 Calc: a User-Friendly Seawater Carbon Calculator for Windows, Max OS X, and iOS (iPhone), U.S. Geological Survey Open-File Report, 2010–1280, pp. 1–17. http://pubs.usgs.gov/of/2010/1280/. accessed 07 November 2018.
Shamberger, K.E.F., Feely, R.A., Sabine, C.L., Atkinson, M.L., DeCarlo, E.H., Mackenzie, F.T., Drupp, P.S., Butterfield, D.A., 2011. Calcification and organic production on a Hawaiian coral reef. Marine Chemistry 64–75. https://doi.org/10.1016/j.marchem.2011.08.003.
Silveira, I., Miranda, L.B., Brown, W.S., 1994. On the origins of the North Brazil current. J. Geophys. Res. 99, 501–512.
Silverman, J., Lazar, B., Erez, J., 2007. Effect of aragonite saturation, temperature, and nutrients on the community calcification rate of a coral reef. J. Geophys. Res. Oceans 112, C05004. https://doi.org/10.1029/2006JC003770.
Soares, M., Paiva, C.C., Freitas, J.E.P., Lotufo, T.M.C., 2011. Gestão de unidades de conservação marinhas: o caso do Parque Estadual Marinho da Pedra da Risca do Meio, NE – Brasil. Rev. Gestão Costeira Integr. 11, 257–268. https://doi.org/10.5894/rgci261.
Soares, M., Martins, F.A.S., Carneiro, P.B.M., Rossi, S., 2017. The forgotten reefs: benthic assemblage coverage on a sandstone reef (Tropical Southwestern Atlantic). J. Mar. Biol. Assoc. U. K. 97, 1585–1592. https://doi.org/10.1017/S002531541600096.
Soares, M., Teixeira, C.E.P., Ferreira, S.M.C., Gurgel, A.L.A.R., Paiva, B.P., Menezes, M.O. B., Davis, M., Tavares, T.C.L., 2019. Thermal stress and tropical reefs: mass coral bleaching in a stable temperature environment? Mar. Biodivers. 49, 2921–2929. https://doi.org/10.1007/s12526-019-00994-4.
Suzuki, A., Nakamori, T., Kayanne, H., 1995. The mechanism of production enhancement in coral reef carbonate systems: model and empirical results. Sediment. Geol. 99, 259—280.
Strickland, J.D.H., Parsons, T.R., 1972. A practical handbook of seawater analysis. Fisheries Research Board of Canada Bulletin, Ottawa.
Suzuki, A., Kawahata, H., 2003. Carbon budget of coral reef systems: an overview of observations in fringing reefs, barrier reefs and atolls in the Indo-Pacific regions. Tellus B 55, 428–444. https://doi.org/10.1034/j.1600-0889.2003.01442.x.
Takahashi, T., Olafsson, J., Goddard, J.G., Chipman, D.W., Sutherland, S.C., 1993. Seasonal variation of CO_2 and nutrients in the high-latitude surface oceans: a comparative study. Global Biogeochem. Cycles 7, 843–878. https://doi.org/10.1029/93GB02263.
Takahashi, T., Sutherland, S.C., Sweeney, C., Poisson, A., Metzl, N., Tilbrook, B., Bates, N., Wanninkhof, R., Feely, R.A., Sabine, C., Olafsson, J., Nojiri, Y., 2002. Global sea-air CO_2 flux based on climatological surface ocean pCO_2, and seasonal biological and temperature effects. Deep Sea Res. Part II 49, 1601–1622. https://doi.org/10.1016/S0967-0645(02)00003-6.
Takahashi, T., Sutherland, S.C., Chipman, D.W., Goddard, J.G., Ho, C., Newberger, T., Sweeney, C., Munro, D.R., 2014. Climatological distributions of pH, pCO_2, total CO_2, alkalinity, and $CaCO_3$ saturation in the global surface ocean, and temporal changes at selected locations. Mar. Chem. 164, 95–125. https://doi.org/10.1016/j.marchem.2014.06.004.
Teixeira, C.E.P., Machado, G.T., 2013. On the temporal variability of the Sea Surface Temperature on the Tropical Southwest Atlantic Continental Shelf. J. Coast. Res. 65, 2071–2076. https://doi.org/10.2112/SI65-350.12013.
Wanninkhof, R., 1992. Relationship between wind speed and gas exchange. J. Geophys. Res. 97, 7373–7382. https://doi.org/10.1029/92JC00188.
Wanninkhof, R., 2014. Relationship between wind speed and gas exchange over the ocean revisited. Limnol Oceanogr. Methods 12, 351–362. https://doi.org/10.4319/lom.2014.12.351.
Ware, J., Smith, S., Reaka-Kudla, M., 1992. Coral reefs: sources or sinks of atmospheric CO2? Coral Reefs 11, 127–130. https://doi.org/10.1007/BF00255465.
Weiss, R.F., 1974. Carbon dioxide in water and seawater: the solubility of a non-ideal gas. Mar. Chem. 2, 203–215. https://doi.org/10.1016/0304-4203(74)90015-2.
Weiss, R.F., Price, B.A., 1980. Nitrous oxide solubility in water and seawater. Mar. Chem. 8, 347–359.

Willeit, M., Ganopolski, A., Calov, R., Brovkin, V., 2019. Mid-Pleistocene transition in glacial cycles explained by declining CO2 and regolith removal. Sci. Adv. 5, 1–9. https://doi.org/10.1126/sciadv.aav7337.

Xue, L., Cai, W., Hu, X., Sabine, C., Jones, S., Sutton, A.J., Jiang, L.-Q., Reimer, J.J., 2016. Sea surface carbon dioxide at the Georgia time series site (2006-2007): air-sea flux and controlling processes. Prog. Oceanogr. 140, 14–26. https://doi.org/10.1016/j.pocean.2015.09.008, 14-26.

Yan, H., Yu, K., Shi, Q., Lin, Z., Zhao, M., Tao, S., Liu, G., Zhang, H., 2018. Air-sea CO_2 fluxes and spatial distribution of seawater pCO_2 in Yongle Atoll, northern-central South China Sea. Continent. Shelf Res. 165, 71–77. https://doi.org/10.1016/j.csr.2018.06.008.